ELSEVIER

Catalysis Today 63 (2000) 517–522

CATALYSIS TODAY

www.elsevier.com/locate/cattod

Deactivation studies over NiO/γ-Al_2O_3 catalysts for partial oxidation of methane to syngas

Yuhong Zhang, Guoxing Xiong*, Shishan Sheng, Weishen Yang

State Key Laboratory of Catalysis, Dalian Institute of Chemical Physics, Chinese Academy of Sciences, Dalian 116023, China

Abstract

Two types of NiO/γ-Al_2O_3 catalysts prepared by the impregnation and the sol–gel method were used for the partial oxidation of methane to syngas at 850°C (GHSV $\sim 1.8 \times 10^5\,\mathrm{l\,kg^{-1}\,h^{-1}}$). The effects of the carbon deposition, the loss and sintering of nickel and the phase transformation of γ-Al_2O_3 support on the catalytic performance during 80 h POM reaction were investigated with a series of characterization such as XRD, BET, AAS, TG, and XPS. The results indicated that the carbon deposition and the loss and sintering of nickel could not cause the serious decrease of catalytic performance over NiO/γ-Al_2O_3 catalyst during the short-time reaction. However, the slow process of the support γ-Al_2O_3 phase transforming into α-Al_2O_3 could slowly decrease the performance of NiO/γ-Al_2O_3 catalysts. Aimed at the reasons of the deactivation, an improved catalyst was obtained by the complexing agent-assisted sol–gel method.

1. Introduction

The nickel-based catalysts are very effective for the partial oxidation of methane to syngas (POM) because of the high turnover rates and inexpensive cost. However, the catalyst deactivates with time on stream by the carbon deposition, the nickel sintering and loss, and by the phase transformation [1]. Lunsford and co-workers [2] reported the serious carbon deposition over the Ni/Al_2O_3 catalyst, which filled the catalyst pores and caused the granules to disintegrate into fine powder at CH_4:O_2 ratios ≥ 2. Schmidt and co-workers [3] found the loss of nickel on the 3 wt.% Ni/Al_2O_3 catalyst during the POM reaction. The CH_4 conversion and H_2 selectivity decreased with 2%.

The deposition of carbonaceous materials may occur over the metallic sites, but also on the acid sites of the support. Tang et al. [4] found that the content of carbon deposition decreased with the increase in base strength of the catalysts for methane reforming with CO_2. We also found that the addition of basic component Li was beneficial to prevent carbon deposition over the nickel-based catalysts [5–7]. In our previous work, it is found that the surface acid centers of γ-Al_2O_3 prepared by sol–gel method are mainly Lewis acid centers, but its acid strength is much weaker than that of normal one [8]. In addition, the stronger interaction between NiO and support on such catalysts is also found in NiO/Al_2O_3 catalysts prepared by sol–gel method, which can restrain the loss and sintering of nickel [9]. These suggest that the resistance of carbon deposition and the sintering of nickel over the supported nickel-based catalysts may be improved by the sol–gel method.

In this work, NiO/γ-Al_2O_3 catalysts prepared by the impregnation and the sol–gel method were tested for POM reaction. A comparative study of the carbon deposition, the loss and sintering of nickel and the support phase transformation was investigated to assess

---

* Corresponding author.
E-mail address: gxxiong@ms.dicp.ac.cn (G. Xiong).

0920-5861/00/$ – see front matter © 2000 Elsevier Science B.V. All rights reserved.
PII: S0920-5861(00)00498-3

the effects of the catalyst preparation method on the catalyst deactivation.

2. Experimental

2.1. Catalyst preparation

Three types of catalysts were used in this study. IT catalyst was prepared by impregnating appropriate amount of $Ni(NO_3)_2$ on commercial γ-Al_2O_3 support. Then dried at 70°C for 12 h and calcined in air at 850°C. ML catalyst was prepared by sol–gel method. The pure 1M AlOOH sol was obtained by peptizing PURAL SB powders (boehmite powders, Condea GmbH, Germany) with nitric acid $(H^+ \text{(mol)}/\text{AlOOH (mol)} = 0.09)$. A correct amount of $Ni(NO_3)_2$ solution was doping into pure AlOOH sol with vigorous stirring to give a homogenous mixture. Drying and calcining are the same as IT catalyst. The improved catalyst named as ML(B) was prepared by the complexing agent-assisted sol–gel method, namely, adding glycerol into AlOOH sol. Other operations were the same as that of ML catalyst. The NiO loading on these catalysts were all about 10 wt.%.

2.2. Test of catalytic performance

Catalysts were tested by flow-reaction in an atmosphere pressure fixed-bed microreactor. The 80 h life test experiments were performed using a microreactor with an internal diameter of 4 mm with 100 mg catalyst employed. The reaction conditions were as follows: $P_{CH_4}{:}P_{O_2} = 2:1$, $GHSV_{CH_4} = 1.8 \times 10^5\,l\,kg^{-1}\,h^{-1}$. The analysis of reaction products was provided elsewhere [6].

2.3. Characterizations of catalysts

X-ray photoelectron spectroscopy (XPS) characterization was performed using a VG ESCA LABMK II spectrometer. The instrument typically operated at pressured below 1.33×10^{-7} Pa and monochromatized Al exciting radiation was used. The binding energy of all spectra was calibrated with respect to the Al_{2p} line at 74.5 eV. The surface relative atomic ratio of catalyst was calculated according to the spectral line intense of XPS [10].

TG test was performed with a Perkin-Elmer 3600 work station at a programmed temperature velocity of $10°C\,min^{-1}$ in air with the flow rate of $25\,ml\,min^{-1}$. The elementary analysis of fresh and aged catalyst samples was carried out in a Perkin-Elmer ICP-5000 apparatus by atomic absorption spectroscopy analysis (AAS).

The specific surface area and pore volume of samples were obtained in a volumetric equipment OMNISORP-100CX by the BET method. X-ray diffraction (XRD) characterization of the catalysts was performed with a Riguku D/Max-RB X-ray diffractometer using a copper target at 40 kV × 100 mA and a scanning speed of $8°\,min^{-1}$.

3. Results and discussion

3.1. Performance of catalysts

The catalytic performances of IT and ML catalysts are shown in Fig. 1. After 10 min initial reaction, the reaction attained steady-state condition. They had CH_4 conversion close to its equilibrium values and high CO selectivity above 97%. It was found that the CH_4 conversion of ML catalyst was slightly lower than that of IT catalyst. These may be due to the sol–gel method that improves the interaction between active component and support, and makes NiO reduce more difficult to Ni^0 [11]. The reduced nickel metal is the active site

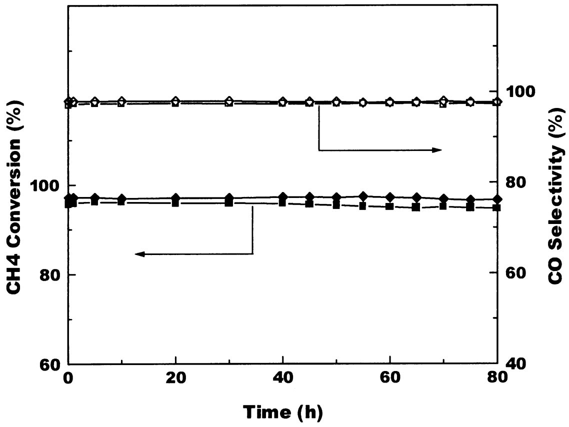

Fig. 1. Performance of catalysts as a function of time ($CH_4/O_2 = 2/1$, GHSV = $1.8 \times 10^5\,l\,kg^{-1}\,h^{-1}$, 850°C, 1 atm) (■) ML catalyst, (◆, ◇): IT catalyst.

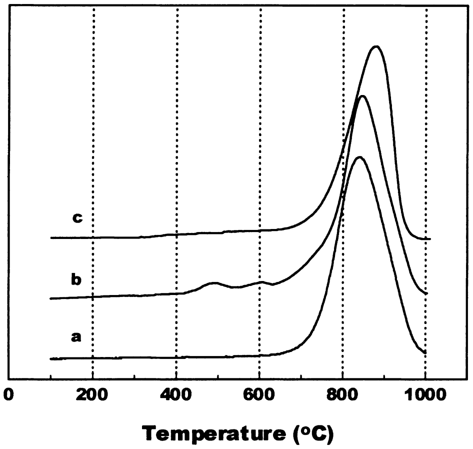

Fig. 2. TPR profiles of (a) $NiAl_2O_4$, (b) IT catalyst and (c) ML catalyst.

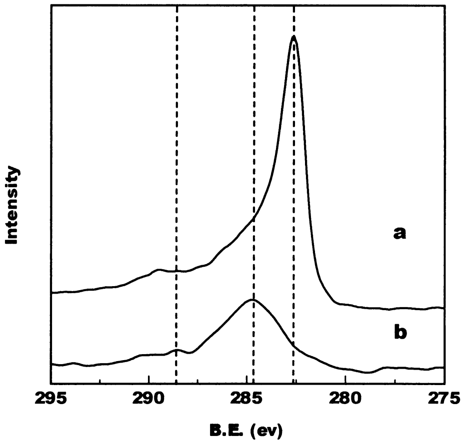

Fig. 3. C_{1s} XPS spectra of catalysts after POM reaction (a) IT catalyst and (b) ML catalyst.

for the POM reaction and POM activity and selectivity are related to the reduction of surface nickel to the reduced state [12]. The TPR profiles also confirmed this result as shown in Fig. 2. The curve of IT catalyst showed a single peak at about 840°C, which was close to the reduction temperature of bulk $NiAl_2O_4$, while the reaction peak of ML catalyst appeared at about 880°C. A rise in reduction temperature over ML catalyst could be attributed to the oxides with stronger interaction with the support.

During the 80 h testing period, no obvious deactivation over the two catalysts was observed. However, CH_4 conversion over ML catalyst decreased slightly after 45 h-testing, but the rate of decrease was very much slow, even not to be easily detected. The decrease value of CH_4 conversion over ML catalysts was less than 1% during the 80 h testing period. At this point, the reaction was stopped and the spent catalysts were analyzed. The results were listed in Table 1. They will be discussed in detail hereinafter.

3.2. Carbon deposition over catalysts

Fig. 3 showed C_{1s} XPS spectra of IT and ML catalysts after 80 h reaction. The binding energy (BE) of 284.6 eV was assigned to adventitious carbon on the surface and the BE of about 283 eV was assigned to surface carbon named as graphite–carbon, which resulted in the pore closing and deactivation of catalyst by covering the nickel surface [13]. The intensity of graphite–carbon over IT catalyst was much stronger than over ML catalyst, which suggested that the amount of surface carbon over IT catalyst was much more than that over ML catalyst. The surface C/Ni atomic ratio of the used IT catalyst increased remarkably to 1.24/0.012 from that of 0.16/0.038 of the fresh IT catalyst. The slight change of the surface C/Ni atomic ratio over the ML catalysts showed that only a little amount of carbon had deposited on the ML catalyst. According to the TG result, the weight of carbon deposition on the IT catalyst was about 17.64% of its

Table 1
The physico-chemical properties of IT and ML catalysts before and after reaction

Sample	Condition	Relative atomic ratio				w (Ni) (%)	w (C) (%)	S ($m^2 g^{-1}$)	V ($ml g^{-1}$)
		C	O	Ni	Al				
IT	Before reaction	0.16	1.55	0.038	1	7.2	–	123.4	28.4
	After reaction	1.24	1.51	0.012	1	6.9	17.64	54.1	12.4
ML	Before reaction	0.20	1.70	0.039	1	8.3	–	111.0	25.5
	After reaction	0.45	1.65	0.031	1	8.2	0.43	32.0	7.4

net weight. However, the weight of surface carbon on the ML catalyst was only 0.43% (nearly negligible). These indicated that the carbon-deposition resistant ability of ML catalyst were much better than that of IT catalyst.

The examination of the IT catalyst surface by scanning electron microscopy (SEM) showed the presence of coke in whiskers. It has been known [14] that coke deposits on Ni catalysts may be present in a variety of morphologies, i.e. amorphous, filamentary (whiskers) and graphitic. The effect of different coke deposit morphologies on the observed catalytic activity can be different, due to the fact that some morphologies do not directly block active sites [15]. Thus, at least for some time, the fraction of coke deposit as whiskers allows the nickel crystalline to remain exposed to the reaction environment, thus retaining their activity. The active sites are deactivated until the rate of carbon formation seriously increases to cover most active sites. Although the carbon deposition were not enough to deactivate IT catalyst during our 80 h testing period, carbon deposition will be a major drawback with Ni-based catalysts during longer reaction period.

3.3. The loss and sintering of nickel over catalyst

The surface relative atomic ratio of catalyst was characterized by XPS (see Table 1). After 80 h reaction, Ni/Al ratio over the used IT catalyst decreased to 0.012 from 0.038 of the fresh one, while the Ni/Al atomic ratio over the used ML catalyst only decreased from 0.039 of the fresh one to 0.031. The results suggested that the loss value of surface nickel of IT catalyst was three times that of ML catalyst or the nickel particles over the IT catalyst was sintered and grew up to decrease the surface area of the nickel particles. Comparing to the change of total nickel content measured with AAS, the loss of total nickel of IT catalyst was 3% while that of ML was only 1%. There results showed that the nickel of IT catalyst lost more seriously than that of ML catalyst. The serious loss and sintering of nickel is an important factor which causes the catalyst deactivation, although the decrease of activity due the loss and sintering of nickel was not observed during 80 h reaction. Therefore, the loss and sintering of nickel could not be disregarded during the period of long-time reaction.

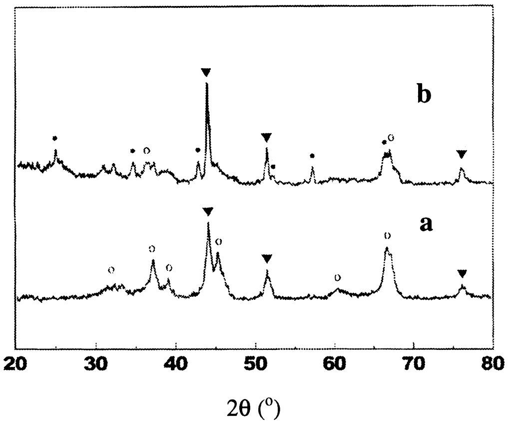

Fig. 4. XRD spectra of IT catalyst (a) before reaction (reduced) and (b) after reaction ((▼) reduced nickel, (●) α-Al_2O_3, (○) γ-Al_2O_3).

3.4. The structure and crystal phase of catalysts

The XRD tests were performed to determine the crystal phases of these catalysts (in Figs. 4 and 5). The fresh catalysts were previously reduced by H_2 at 850°C before XRD test. Their XRD spectra were similar, only γ-Al_2O_3 appeared except for reduced nickel phase. After 80 h experiment, it was found that the intensity of XRD patterns of reduced nickel over spent ML catalyst was lower than that over spent IT catalyst (see Figs. 4b and 5b), which suggested that ML

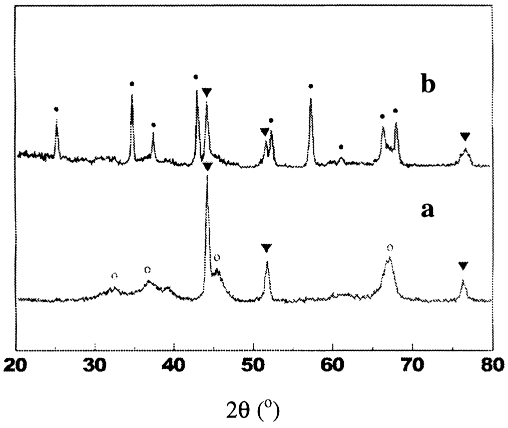

Fig. 5. XRD spectra of ML catalyst (a) before reaction (reduced) and (b) after reaction ((▼) reduced nickel, (●) α-Al_2O_3, (○) γ-Al_2O_3).

catalyst could inhibit the sintering of metal nickel over catalysts.

Compared the XRD spectra of used catalysts with fresh catalysts, respectively, it revealed the different sintering behaviors of support over the different catalysts. The XRD spectrum of the used IT catalyst was similar to that of fresh catalyst, and only a little α-Al_2O_3 appeared except for γ-Al_2O_3 and reduced nickel phase. However, the XRD spectrum of the used ML catalyst was different from that of the fresh catalyst, γ-Al_2O_3 phase of support disappeared completely and transformed into α-Al_2O_3 phase. Compared with the specific surface area of catalyst before reaction (see Table 1), the surface area of IT catalyst after reaction decreased by 56%, while the surface area of ML catalyst after reaction decreased by 71%. These results suggested that the support structure of ML catalyst was unstable and sintered to α-Al_2O_3 during POM reaction.

The XRD of fresh catalysts (unreduced) were a mixture of spinel and γ-Al_2O_3. Formation of α-Al_2O_3 from the spent catalyst under POM reaction conditions could probably be explained by the fact that some of the Ni^{2+} in spinel might be reduced to metallic nickel which fall out of the spinel structure and then the part containing the nickel-less lattice converted to α-Al_2O_3 [16]. Smaller pores of the catalysts and supports prepared by sol–gel accelerated the sintering of support. The decrease of CH_4 conversion over ML catalyst after 45 h reaction was caused by the transformation of support γ-Al_2O_3 into α-Al_2O_3. The phase transformation was a slow process so that the decrease of activity was very slow as observed.

3.5. The improved catalysts prepared by the sol–gel method

The above results suggested that a NiO/γ-Al_2O_3 catalyst either with a high resistance of the carbon deposition and the loss and sintering of nickel or with a better thermal stability of support could be obtained if the phase transformation of γ-Al_2O_3 support on the catalysts prepared by the sol–gel method could be inhibited. Masuda et al. [17] found that the thermostability of γ-Al_2O_3 could be improved by the complexing agent-assisted sol–gel method. So an improved catalyst was obtained by such way. Fig. 6 showed the XRD spectra of the different fresh catalyst calcined at 1200°C for 5 h and the used catalyst. It was found that the phase of the improved catalyst was very stable and no phase transformed even after calcined for 5 h at 1200°C, while the part of γ-Al_2O_3 supports on the

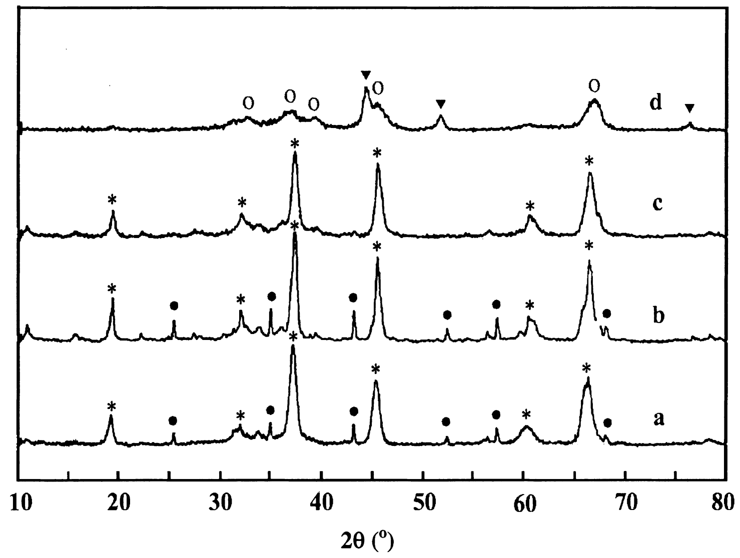

Fig. 6. XRD spectra of the catalysts (a) IT, (b) ML, (c) ML(B) and (d) the used ML(B) ((a)–(c) after calcining at 1200°C for 5 h, (d) ML(B) catalyst after 80 h reaction). (▼) Reduced nickel, (●) α-Al_2O_3, (○) γ-Al_2O_3, (*) $NiAl_2O_4$.

IT and ML catalysts have transformed into α-Al_2O_3. After 80 h reaction, no α-Al_2O_3 phase appeared and the surface area was still kept above 77 $m^2\,g^{-1}$. On the other hand, the catalytic performance of the improved catalyst could also be kept stable during the period of 80 h reaction. This part work will be reported in other paper in detail.

4. Conclusion

The carbon deposition, the loss and sintering of nickel and the phase transformation are important factors to deactivate the NiO/γ-Al_2O_3 catalysts. The catalyst prepared by sol–gel method exhibited an excellent ability to resistant carbon deposition and to inhibit the loss and sintering of nickel. However, its support (γ-Al_2O_3) was unstable under POM reaction condition and transformed into α-Al_2O_3, which caused a very slow decrease of CH_4 conversion. By the complexing agent-assisted sol–gel method, the phase transformation of the support can be inhibited to obtain a stable NiO/γ-Al_2O_3 catalyst for POM.

Acknowledgements

The project was supported by the National Sciences Foundation of China (Grant number 29392003) and by Chinese Academy of Sciences (Grant number KJ951-A1-508-2).

References

[1] C.H. Bartholomew, R.B. Pannell, R.W. Fowler, J. Catal. 79 (1983) 34.
[2] D. Dissanayake, M.P. Rosenek, K.C.C. Kharas, J.H. Lunsford, J. Catal. 132 (1991) 117.
[3] P.M. Torniainen, X. Chu, L.D. Schmidt, J. Catal. 146 (1994) 1.
[4] S.B. Tang, F.L. Qiu, S.J. Lu, Catal. Today 24 (1995) 253.
[5] G.X. Xiong, Q. Miao, China Patent, Application No. 9511007.8 (1995).
[6] Q. Miao, G. Xiong, S. Sheng, W. Cui, L. Xu, X. Guo, Appl. Catal. A 154 (1997) 17.
[7] S. Liu, G. Xiong, S. Sheng, Q. Miao, W. Yang, Stud. Surf. Sci. Catal. 111 (1998) 747.
[8] M. Lu, G. Xiong, J. Gu, H. Zhao, H. Bauser, in: Proceedings of the International Symposium on Membranes and Membrane Processes (ISMMP'94), (1994) 449.
[9] Y. Zhang, G. Xiong, S. Sheng, S. Liu, W. Yang, Acta Physico-chem. Sinica 15 (8) (1999) 735.
[10] Y. Boudevilie, F. Figueras, J-L. Portefaix, J.C. Vedrine, J. Catal. 58 (1979) 52.
[11] J.R.H. Ross, M.C.F. Steel, A. Zeini-Isfahani, J. Catal. 52 (1978) 280.
[12] Q. Miao, G. Xiong, S. Sheng, W. Cui, X. Guo, Stud. Surf. Sci. Catal. 101 (1996) 453.
[13] D.L. Trimm, Catal. Rev.-Sci. Eng. 21 (1987) 155.
[14] R.T.K. Baker, M.A. Barber, P.S. Harris, F.S. Feates, R.I.J. Waite, J. Catal. 26 (1992) 51.
[15] J.A. Peña, J. Herguido, C. Guimon, A. Monzón, J. Santamatiá, J. Catal. 159 (1996) 313.
[16] A. Bhattacharyya, V.W. Chang, Stud. Surf. Sci. Catal. 88 (1994) 207.
[17] K. Masuda, T. Sano, F. Mizukami, T. Takezaki, K. Kuno, Appl. Catal. B 4 (1994) 187.